Hindawi
International Journal of Aerospace Engineering
Volume 2022, Article ID 6900904, 15 pages
https://doi.org/10.1155/2022/6900904

Research Article

Distributed Control Design for Uncertain Multiagent Systems with Heterogenous High Powers

Hanqiao Huang,[1] Hantong Mei,[2] Di Zhang,[3] Yunhe Guo,[3] and Ge Zhou[3]

[1]*Unmanned System Research Institute, Northwestern Polytechnical University, Xi'an, China*
[2]*School of Astronautics, Northwestern Polytechnical University, Xi'an, China*
[3]*Shanghai Electro-Mechanical Engineering Institute, Shanghai, China*

Correspondence should be addressed to Hantong Mei; may.mht@mail.nwpu.edu.cn

Received 5 March 2022; Revised 1 June 2022; Accepted 13 June 2022; Published 8 July 2022

Academic Editor: Chen Pengyun

In this paper, a distributed asymptotic tracking control strategy is investigated by establishing filters and barrier function-based consensus control scheme to address the control of heterogenous power-chained multiagent systems (MASs) under a directed graph subject to the unknown input deadzone nonlinearities and unknown control coefficients. First, to generate estimation information from the leader, a two-order filter is exploited for every agent which solves the difficultly of the time-varying control coefficients in multiagent systems with a directed topology. Then, based on the two-order filters, prescribed performance method and barrier functions are utilized to establish the distributed tracking protocol to handle the power-chained deadzone input nonlinearities, such that the MAS can reach the global consensus while guaranteeing the prescribed tracking error performance. Using the Lyapunov stability theorem, the proof of the convergence is accomplished rigorously. Ultimately, the efficacy and advantage of the devised method are validated by two simulation examples.

1. Introduction

The problem of distributed control for nonlinear MASs has been investigated for several decades, and a lot of significant achievements have been achieved [1–4]. Recently, various control methodologies, including the function approximation control techniques [5], adaptive control [6], and robust control [7], have been studied extensively for nonlinear MASs. In [8, 9], a consensus tracking protocol for uncertain pure feedback MASs is addressed. The distributed tracking problem based on observer is studied for nonlinear MASs with uncertain networks in [10]. In [11], on the strength of Nussbaum-type gain technique, both leaderless and leader-following consistent tracking control methodologies can make the errors converge be guaranteed asymptotically to zero for a second-order MAS with unknown control directions, without any information about the global communication graph. Under directed topologies or undirected topologies, a distributed adaptive control approach is applied to the leader-following networked Lagrangian systems with unknown control directions in [12]. However, the leader-following system assumes that there is only one leader in the system, and the communication graph among the followers is an undirected connected topology. Different from adaptive designs, [13] proposes a prescribed performance control method for an uncertain multiagent system. For resolving the consensus difficulty in MASs with unknown nonlinearities, neural networks or fuzzy logic systems are used as universal approximators in [14–16]. To settle the issue of unknown control directions, [17] presents a novel Nussbaum-type function. Although these above studies can obtain good command tracking performance, there is still a lack of research on fault-tolerant control design.

From a practical perspective, input deadzone nonlinearity is one of the key problems in nonlinear control system design, which results in the unaccomplished desired control efforts [18]. In the process of multiagent control design, if the control input constraints are not considered, the closed-loop system may be limited by performance and even lose stability. Therefore, the control investigations on

restricted MASs has already attracted extensive attention in recent years [19]. On the basis of meeting preset trigger conditions, in [20], a distributed adaptive control approach is investigated for the uncertain MAS to deal with intermittent actuator faults. By introducing a predictor to obtain each error surface estimation, a distributed adaptive fuzzy consensus tracker design is used for MASs with input saturations [21]. In [22], the time-varying formation tracking control protocol for multileader MASs is studied in order to address the problem of actuator failure and saturation nonlinearity simultaneously. Whereas, the augmented plant of [22] is constructed complicatedly, and the first-order low-pass filter greatly increases the uncertainty of numerical simulation results. To compensate for both actuator bias fault and loss of actuator effectiveness fault, a fully distributed control scheme is constructed in [23]. In [24], a fully distributed protocol based on prescribed performance control is proposed to set predefined overshoot range, guarantee convergence rates, and limit neighbourhood synchronization steady-state errors for uncertain nonlinear MASs with deadzone inputs. Despite the workload of [24] is very sufficient and it is greatly improved compared with other aforementioned papers, the proposed strategy is still limited in the scope to the unity low power of MASs. As a matter of fact, there are a lot of practical heterogenous power-chained MASs, such as the coupled underactuated unstable 2-DOF machinery model (i.e., equation (38)) of [25] and the roll dynamic model of multiple axisymmetric skid to turn missiles as Example 2 of [26]. Thus, it is of necessity to do the research on MASs with heterogenous high powers. However, most control approaches applied to date have been limited in their boundary to the unity low power of MASs owing to the uncontrollable linearization of nonlinear systems caused by the high-power chains of control variables.

Contrary to these, the distributed consensus control for power-chained MASs with limited communication networks is seldom studied. Based on the controller of single nonlinear power-chained systems, aiming at the networked nonlinear power-chained MASs, [27] proposes a robust cooperative output tracking control protocol. Adding a power integrator technique and adaptive disturbance compensator are introduced to reduce the degradation of system performance for complex nonlinear MASs with input noise in [28]. By utilizing the distributed integrator backstepping approach, the boundness of the closed-loop system for multiple strict-feedback stochastic nonlinear systems under a directed leader-followers type communication graph is achieved in [29]. In [30], a neural adaptive tracking control scheme is employed to nonstrict feedback nonlinear MASs. A distributed low-complexity control strategy is proposed in [26] to guarantee consensus tracking performance of uncertain heterogenous power-chained MASs. We note that considerable progress has been made in the distributed control of MASs, but there are still some nonnegligible issues that need to be solved. First, for MASs with high powers, there are some restrictions on the heterogenous high powers. Specifically, the existing design methods usually require the high powers to be identical or to be known for establishing the control protocols. For example, in order to enable the control design for high power systems, [26] assumes the powers of the first order to be known (i.e., see Assumption 3 in [26]). Second, for MASs with a directed communication graph, the existing approaches do not consider the control coefficients or require that the control coefficients must be constants. The reason making it difficult is that the directed graph Laplace matrix is asymmetric. Considering the time-varying control coefficients of MASs are unknown, traditional adaptive control techniques [3, 20] used to address the time-varying coefficients will make the unknown matrix P inestimable, where P is defined by the Laplacian matrix and the communication directed matrix (i.e., see Lemma 1 in [5]). To circumvent the difficulties, the symmetric positive definite property of Laplacian matrix between followers is implicitly used in most theoretical analyses [24]. Whereas, this means that these methods are not applicable to the MAS with a directed topology. Third, there is no performance envelope scheme to predetermine the distributed consensus tracking error in the controller design of MASs with heterogeneous unknown uncertain powers. Moreover, it should be stressed out that the global control of heterogenous power-chained MASs with unknown input deadzone nonlinearities and unknown control coefficients is still an unsolved problem.

Inspired by the aforementioned discussion, the paper proposes the design of a distributed control for uncertain MASs with a directed graph. Compared to the relevant existing researches in the literature, the main contributions of this paper can be concluded as follows.

(1) The investigated control scheme is able to relax the aforementioned four restrictions in the existing consensus researches [26–30] for power-chained MASs with input deadzone nonlinearities

(2) To deal with the time-varying difficulty of multiagent control coefficients, a second-order filter is exploited to make each agent generate the estimations of the leader signals, thus avoiding to use the asymmetric Laplacian matrix of the directed topology

(3) To solve the unknown nonlinearities in MAS, barrier functions are applied to the prescribed tracking distributed protocol, which make the specified tracking performance guaranteed; thus, the convergence of the controlled system is proved, and all the closed signals are globally bounded

2. Problem Formulation

2.1. Problem Statement. In this subsection, the analysis on control system with nonlinear deadzone is given first. Then, the new mathematical model under nonlinear model with asymmetric deadzone is constructed.

In practical physical systems, certain abnormal events and emergencies may happen in time of operation, which

will result in the failure of the actuator. Besides, as a result of the practical constraints on manufacturing and assembly process, the actual output of actuators often presents the characteristic of asymmetric deadzone nonlinearity. The actual control input nonlinear model can be modelled as follows.

$$D(t,u)=\begin{cases} h_r(t)(u-b_r), & u\geq b_r,\\ 0, & b_l<u<b_r,\\ h_l(t)(u-b_l), & u\leq b_l, \end{cases} \tag{1}$$

where $u\in\mathbb{R}$ is the control input, $D(t,u)$: $\mathbb{R}\longrightarrow\mathbb{R}$ is the control output with nonlinear deadzone, $h_r(t)$ and $h_l(t)$ are unknown time-varying positive continuous functions denoting the left and right slopes of the deadzone, $b_l<0$ and $b_r>0$ are unknown parameters representing the break-points of deadzone nonlinearity, as shown in Figure 1.

According to (1), for the purpose of facilitating the control law design, the deadzone function can be modelled as

$$D(t,u)=h(t)u+d(t,u), \tag{2}$$

with

$$h(t)=\begin{cases} h_l(t) & \text{if } u\leq 0\\ h_r(t) & \text{if } u>0 \end{cases}, d(t,u)=\begin{cases} -h_r(t)b_r & \text{if } u\geq b_r,\\ -h(t)u & \text{if } b_l<u<b_r,\\ -h_l(t)b_l & \text{if } u\leq b_l. \end{cases} \tag{3}$$

The uncertain high-order nonlinear MASs with Nn-th order agents can be modelled by the following dynamic equations

$$\begin{aligned} &\dot{x}_{k,i}=f_{k,i}(t,\bar{x}_{k,i})+g_{k,i}(t,\bar{x}_{k,i})x_{k,i+1}^{p_{k,i}},\ i=1,\cdots,n-1,\\ &\dot{x}_{k,n}=f_{k,n}(t,\bar{x}_{k,n})+g_{k,n}(t,\bar{x}_{k,n})(h_k(t)u_k+d_k(t,u))^{p_{k,n}},\\ &y_k=x_{k,1},\quad k=1,\cdots,N, \end{aligned} \tag{4}$$

where $\bar{x}_k=[x_{k,1},\cdots,x_{k,n}]^T\in\mathbb{R}^n$ are the states with initial conditions $\bar{x}_k^0=[x_{k,1}(0),\cdots x_{k,n}(0)]^T$, $\bar{x}_{k,i}=[x_{k,1},\cdots,x_{k,i}]^T\in\mathbb{R}^i$, $x_i=[x_{1,i},\cdots,x_{N,i}]^T\in\mathbb{R}^N$, $x_i^{p_i}=[x_{1,i}^{p_i},\cdots,x_{N,i}^{p_i}]^T\in\mathbb{R}^N$, $u_k\in\mathbb{R}$ is the actual control input, $y_k\in\mathbb{R}$ is the output; $p_{k,i}\geq 1$ is all unknown odd integers. The system nonlinearities $f_{k,i}(t,\bar{x}_{k,i})$, $g_{k,i}(t,\bar{x}_{k,i})$: $\mathbb{R}\times\mathbb{R}^i\longrightarrow\mathbb{R}$ and $i=1,\cdots,n$ are unknown continuous functions of $\bar{x}_{k,i}(t)$. Without loss of generality, the unknown control coefficients $g_{k,i}(t,\bar{x}_{k,i})$ are supposed to be strictly positive.

The desired trajectory for the subsystem output $y_d(t)$ is bounded and known only to some subsystems, and $\dot{y}_d(t)$ is bounded and unknown to all subsystems.

The goal of the paper is to design a distributed tracking protocol for the multiagent system (4) with heterogenous high powers under the directed graph, so that all the agents' output tracking errors (i.e., $|y_k-y_d|$, $k=1,\cdots,N$) converge to the predesigned transient and steady state performance boundaries, and simultaneously, make sure all signals of the closed loop system bounded.

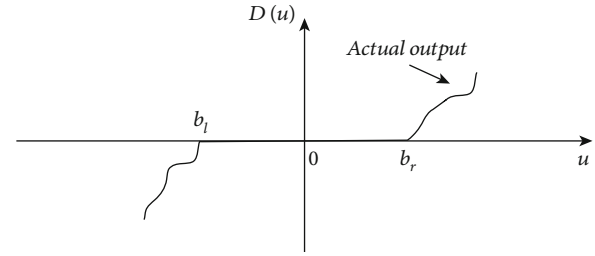

Figure 1: A typical example of thinking about deadzone classes.

2.2. Algebraic Graph Theory. Let the telecommunication network among agents be denoted by a directed graph $\mathcal{G}=(\mathcal{V},\mathcal{E},\mathcal{A})$, where $\mathcal{V}=\{v_1,v_2,\cdots,v_n\}$ represents the index set corresponding to each node with v_i being the i-th agent, $\mathcal{E}\subseteq\mathcal{V}\times\mathcal{V}$ represents the set of the edges, $\mathcal{A}=[a_{ij}]$ represents the adjacency matrix. (i,j) denotes an edge of the graph $\mathcal{G}$, and $(i,j)\in\mathcal{E}$ indicates that there is an agent j-to-agent i communication. The element a_{ij} of $\mathcal{A}$ corresponding to the edge (i,j) represents the quality of communication between the agents i and j (i.e., $(i,j)\in\mathcal{E}\Leftrightarrow a_{ij}>0$), otherwise, $a_{ij}=0$. $\mathcal{G}$ is referred to as an undirected graph if and only if $a_{ij}=a_{ji}$. Stipulate that the diagonal elements $a_{ii}=0$. Clearly, for a directed graph, $\mathcal{A}$ is unsymmetrical. The in-degree matrix $\mathcal{D}=\text{diag}(\mathcal{D}_i)\in\mathbb{R}^{N\times N}$, with $\mathcal{D}_i=\sum_{j=1}a_{ij}$ being the i-th row sum of $\mathcal{A}$. Moreover, the Laplacian matrix $\mathcal{L}=[l_{ij}]\in\mathbb{R}^{N\times N}$ for the directed digraph $\mathcal{G}$ can be defined as $\mathcal{L}=\mathcal{D}-\mathcal{A}$. Besides, defining $\mathcal{B}=\text{diag}\{b_i\}\in\mathbb{R}^{N\times N}$ to denote the communication directed topology between the agents and the desired trajectory y_d, where $b_i=1$ means that y_d is directly accessible by agent i, otherwise, $b_i=0$. A sequence of edges in a graph $\mathcal{G}$ of the form $\{(i,i_1),(i_1,i_2),(i_2,i_3),(i_3,i_4)\}$ is called a path. The following notation is utilized over all the paper. Have $a\in\mathbb{R}^n$ and $b\in\mathbb{R}^n$ being two vectors, next, a vector operator $.*$ is defined as $a.*b=[a(1)b(1),\cdots,a(n)b(n)]^T$.

Assumption 1. The directed graph $\mathcal{G}=(\mathcal{V},\mathcal{E},\mathcal{A})$ includes a directed spanning tree, and the desired trajectory $y_d(t)$ is accessible to at least one subsystem.

Assumption 2. There are unknown and continuous functions $\widehat{h}_k(\cdot)$: $\mathbb{R}\longrightarrow(0,\infty)$ and nonnegative $\widehat{d}_k(\cdot)$: $\mathbb{R}\longrightarrow[0,\infty)$ such that $|h_k(t,u)|\leq\widehat{h}_k(u)$ and $|d_k(t,u)|\leq\widehat{d}_k(u)$.

Lemma 3 (see [1]). *For any real number y, time-varying function $a(t)$ in field of real number and any odd integer $p\geq 1$, the*

following inequality is always true

$$y\left((-y+a(t))^p - a(t)^p\right) \le -\frac{y^{p+1}}{2^{p-1}}. \tag{5}$$

Lemma 4 (see [31]). *Let q and w be real variables. Then, for any integers $a > 0$, $b > 0$ and any real number $\varepsilon > 0$, the following inequality is always true*

$$|q|^a|w|^b \le \frac{a}{a+b}\varepsilon|q|^{a+b} + \frac{b}{a+b}\varepsilon^{-a/b}|w|^{a+b}. \tag{6}$$

Remark 5. Assumption 1 and Assumption 2 are not violated conditions. Under a directed topology, the expected trajectory $y_d(t)$ can only be accessible to a subset of followers (i.e., $\sum_{i=1}^{N} b_i > 0$) in Assumption 1. In Assumption 2, $h_k(t)$ denotes the left and right slopes of the deadzone when $u \le b_l$ and $u \ge b_r$ (i.e., when $u \le b_l$ and $u \ge b_r$, $h_k(t) = \partial D_k(t, u_k)/\partial u_k$). In engineering practice, the slope is usually bounded, because for any real physical system, the slope of the control input cannot be infinite, which means that there must be an upper bound of $h_k(t)$. Simultaneously, the unknown input nonlinearity function $d_k(t, u)$ is bounded obviously due to the upper boundness of $h_k(t)$. Besides, it is usually supposed that $|\partial D(t, u)/\partial u| > 0$ (i.e., see Assumption 2 in [32]), but this assumption cannot be satisfied when there are unknown deadzone nonlinearities because the derivative between the breakpoints is zero [24], (i.e., $\partial D_k(t, u_k)/\partial u_k = 0$, for $b_l < u_k < b_r$). In this work, when $b_l \le u \le b_r$, $h_k(t) \ne \partial D_k(t, u_k)/\partial u_k$ (i.e., the aforementioned positive nature requirement on $h_r(t)$, $h_l(t)$ will not restrict a zero value appearing in the dead-band as $\partial D_k(t, u_k)/\partial u_k = 0$). Therefore, Assumption 2 is realistic and reasonable.

Remark 6. In this paper, the time-varying system nonlinearities $f_{k,i}$ and $g_{k,i}$ are unknown continuous functions, such that little knowledge can be used to establish the control scheme. To handle the difficulty, neural networks and fuzzy logic [14–16] are utilized for approximating the unknown functions as a consequence of the system nonlinearities $f_{k,i}(t, \bar{x}_{k,i})$ and $g_{k,i}(t, \bar{x}_{k,i})$. But only semiglobal results can be got due to the employment of the approximators. It is a challenge problem to establish a distributed protocol for the unknown nonlinear MASs with global consensus, which will be solved skillfully by cooperating two-order filters and barrier functions as follows.

3. Main Results

In this section, first, we design a filter $(q_{k,1}, q_{k,2})$ for each agent to generate estimate information from the leader. Subsequently, a distributed asymptotic tracking controller for an uncertain MAS with deadzone input nonlinearities and heterogenous high powers will be designed. Finally, we shall demonstrate that it results in the solution for the problem of predesigned performance for (4).

3.1. Filter Design. To facilitate the distributed control design, a filter $(q_{k,1}, q_{k,2})$ is utilized for each agent k, where $k = 1, \cdots, N$.

Denote

$$z_{k,p} = b_k\left(q_{k,p} - y_d^{(p-1)}\right) + \sum_{j=1}^{N} a_{kj}\left(q_{k,p} - q_{j,p}\right), p = 1, 2, \tag{7}$$

where $y_d^{(0)} = y_d$, $y_d^{(1)} = \dot{y}_d$. Then, design the filters as

$$\begin{cases} \dot{q}_{k,1} = q_{k,2}, \\ \dot{q}_{k,2} = \alpha_k, \end{cases} \tag{8}$$

with

$$\alpha_k = -c_2 z_{k,1} - c_1 z_{k,2} - c_0 q_{k,2} - c_0 \text{ sgn } (\underline{z}_k) \sum_{p=1}^{2} \widehat{F}_{k,p}, \tag{9}$$

$$\begin{cases} \dot{\widehat{F}}_{k,1} = b_k(F_{k,1} - y_d) + \sum_{j=1}^{N} a_{kj}\left(\widehat{F}_{k,1} - \widehat{F}_{j,1}\right), \\ \dot{\widehat{F}}_{k,2} = b_k(F_{k,2} - \dot{y}_d) + \sum_{j=1}^{N} a_{kj}\left(\widehat{F}_{k,2} - \widehat{F}_{j,2}\right), \end{cases} \tag{10}$$

where c_0, c_1, and c_2 are positive constant parameters selected as $c_0 \ge 1$, $c_1 > c_0 + 1$, and $c_2 = c_0 c_1$, $F_{k,1}$ is the upper boundary of $|y_d|$, $F_{k,2}$ is the upper boundary of $|\dot{y}_d|$, $k = 1, \cdots, N$.

Theorem 7. *Consider a closed-loop system composed of N filters (8) under Assumption 1 with control design (9). The asymptotic and consistent tracking of all outputs of the filter to $y_d(t)$ can be realized (i.e., $\lim_{t \longrightarrow +\infty} |q_{k,1} - y_d(t)| = 0$, $k = 1, \cdots, N$). In addition, $q_{k,1}$ and $q_{k,2}$ are bounded.*

Proof. Based on Assumption 1, the matrix $\mathcal{L} + \mathcal{B}$ is nonsingular. Same as [5], define $\theta = [\theta_1, \cdots, \theta_N]^T = (\mathcal{L} + \mathcal{B})^{-1}[1, \cdots, 1]^T$, $\mathcal{P} = \text{diag}\{P_1, \cdots, P_N\} = \text{diag}\{\theta_1^{-1}, \cdots, \theta_N^{-1}\}$, $\mathcal{Q} = \mathcal{P}(\mathcal{L} + \mathcal{B}) + (\mathcal{L} + \mathcal{B})^T\mathcal{P}$, where $\theta_k > 0$ for $k = 1, \cdots, N$. It can be summarized from [5] that $\mathcal{Q}$ is positive definite.

Construct the following Lyapunov function

$$V_z = \frac{1}{2} z^T \mathcal{P} z + \frac{1}{2\gamma} \sum_{p=1}^{2} \tilde{F}_p^T \mathcal{P} \tilde{F}_p, \tag{11}$$

where $z = [\underline{z}_1, \underline{z}_2, \cdots, \underline{z}_N]^T \in \mathbb{R}^N$ with $\underline{z}_k = c_0 z_{k,1} + z_{k,2}$, $\widehat{F}_p = [\widehat{F}_{1,p}, \widehat{F}_{2,p}, \cdots, \widehat{F}_{N,p}]^T \in \mathbb{R}^N$, $F_p = [F_{1,p}, F_{2,p}, \cdots, F_{N,p}]^T \in \mathbb{R}^N$, $\tilde{F}_p = \widehat{F}_p - F_p \in \mathbb{R}^N$, $p = 1, 2$, and $\gamma > 0$ is a constant satisfying $\gamma < 2\lambda_{\min}^2(\mathcal{Q})/\varphi^2$ with $\varphi = \|\mathcal{P}(\mathcal{L} + \mathcal{B})\| \in \mathbb{R}$. Denote $z_p = [z_{1,p}, z_{2,p}, \cdots, z_{N,p}]^T \in \mathbb{R}^N$, $\alpha = [\alpha_1, \alpha_2, \cdots, \alpha_N]^T \in \mathbb{R}^N$, and $q_p = [q_{1,p}, q_{2,p}, \cdots, q_{N,p}]^T \in \mathbb{R}^N$, $p = 1, 2$. Then, the following

equation can be obtained

$$\dot{z} = (\mathscr{L} + \mathscr{B})(c_0 q_2 + \alpha - c_0 \dot{y}_d - \ddot{y}_d). \tag{12}$$

Through (11) and (12), by denoting $\operatorname{sgn}(\underline{z}) = [\operatorname{sgn}(\underline{z}_1), \cdots, \operatorname{sgn}(\underline{z}_N)]^T$, the time derivative of V_z is

$$\begin{aligned}
\dot{V}_z &= z^T \mathscr{P}(\mathscr{L} + \mathscr{B}) \left(-c_1 z - c_0 \sum_{p=1}^{2} \operatorname{sgn}(\underline{z}) .* F_p + c_0 \sum_{p=1}^{2} \varepsilon(\underline{z}) .* F_p - c_0 \dot{y}_d - \ddot{y}_d \right) \\
&\quad - \frac{1}{\gamma} \sum_{p=1}^{2} \tilde{F}_p^T \mathscr{P}(\mathscr{L} + \mathscr{B}) \tilde{F}_p \le -c_1 z^T \mathscr{Q} z - \frac{1}{\gamma} \sum_{p=1}^{2} \tilde{F}_p^T \mathscr{Q} \tilde{F}_p \\
&\quad - c_0 \sum_{p=1}^{2} z^T \mathscr{P} \mathscr{D} \operatorname{sgn}(\underline{z}) .* F_p + c_0 \sum_{p=1}^{2} z^T \mathscr{P} \mathscr{A} \operatorname{sgn}(\underline{z}) .* F_p \\
&\quad - c_0 \sum_{p=1}^{2} z^T \mathscr{P} \mathscr{B} \operatorname{sgn}(\underline{z}) .* F_p - \sum_{p=1}^{2} z^T \mathscr{P}(\mathscr{L} + \mathscr{B})(c_0 \dot{y}_d + \ddot{y}_d) \\
&\quad + c_0 \sum_{p=1}^{2} \|z\| \|\mathscr{P}(\mathscr{L} + \mathscr{B})\| \|\tilde{F}_p\|.
\end{aligned} \tag{13}$$

It should be noticed that $c_0 \sum_{p=1}^{2} z^T \mathscr{P} \mathscr{D} \operatorname{sgn}(z) .* F_p = c_0 \sum_{p=1}^{2} F_p \sum_{j=1}^{N} p_j a_{ij} |\underline{z}_j|$, $c_0 \sum_{p=1}^{2} z^T \mathscr{P} \mathscr{A} \operatorname{sgn}(z) .* F_p \le c_0 \sum_{p=1}^{2} F_p \sum_{j=1}^{N} p_j a_{ij} |\underline{z}_j|$, $c_0 \sum_{p=1}^{2} z^T \mathscr{P} \mathscr{B} \operatorname{sgn}(z) .* F_p = c_0 \sum_{p=1}^{2} F_p \sum_{j=1}^{N} p_j b_j |\underline{z}_j|$, $\sum_{p=1}^{2} |z^T \mathscr{P}(\mathscr{L} + \mathscr{B})(c_0 \dot{X}_d + \ddot{X}_d)| \le c_0 \sum_{p=1}^{2} F_p \sum_{j=1}^{N} p_j \mu_j |\underline{z}_j|$, and $\sum_{p=1}^{2} \|z\| \|\mathscr{P}(\mathscr{L} + \mathscr{B})\| \|\tilde{F}_p\|^2 + \sum_{p=1}^{2} \varphi^2 \|\tilde{F}_p\| / 2\lambda_{\min}(\mathscr{Q})$, with $\lambda_{\min}(\mathscr{Q})$ representing the minimum eigenvalue of $\mathscr{Q}$.

Combing these above inequality, (13) becomes

$$\dot{V}_z \le -c_2 \|z\|^2 - \gamma^* \|\tilde{F}_p\|, \tag{14}$$

where $c_2 = \lambda_{\min}(\mathscr{Q})(c_1 - c_0)$, $\gamma^* = \lambda_{\min}(\mathscr{Q})(1/\gamma - \varphi^2 / 2\lambda_{\min}^2(\mathscr{Q}))$. It is easy to verify that $c_2 > 0$ and $\gamma^* > 0$. Thus, it can be obtained from (14) that $\lim_{t \to +\infty} \|z\| = 0$ and $\lim_{t \to +\infty} |q_{k,1}(t) - y_d(t)| = 0$ accordingly, $k = 1, \cdots, N$. The boundedness of $q_{k,1}$ and $q_{k,2}$ can be deduced on the basis of the boundedness of V_z and $\|z\|$. The proof is completed. □

3.2. Control Scheme. In this subsection, the distributed tracking control scheme is constructed cooperating with the filter (8). We define the error variables $e_{k,i} \in \mathbb{R}$, $k = 1, \cdots, N$, and $i = 1, \cdots, n$ as

$$e_{k,1} = x_{k,1} - q_{k,1}, \tag{15}$$

$$e_{k,i} = x_{k,i} - v_{k,i}, i = 2, \cdots, n, \tag{16}$$

where $v_{k.i}$ is the intermediate control signal, which will be defined later.

Define $\rho_i = [\rho_{1,1}, \cdots, \rho_{N,1}]^T \in \mathbb{R}^N$ and select an output performance function for $t \ge 0$

$$\rho_{k,i}(t) = \left(\rho_{k,i}^0 - \rho_{k,i}^\infty\right) \exp(-l_{k,i} t) + \rho_{k,i}^\infty, \tag{17}$$

where $k = 1, \cdots, N$, $i = 1, \cdots, n$ and the constant design parameters $l_{k,i} > 0$, $\rho_{k,i}^0 = \rho_{k,i}(0) > 0$, and $\rho_{k,i}^\infty = \lim_{t \to \infty} \rho_{k,i}(t) > 0$ are chosen appropriately to satisfy $\rho_{k,i}^0 > \rho_{k,i}^\infty$ and $|e_{k,i}(0)| < \rho_{k,i}^0$ with any given initial condition $\bar{x}_{k,i}(0)$.

Define the barrier functions $t \mapsto r_{k,i}(t)$ as

$$r_{k,i}(t) = \ln\left(\frac{1 + \xi_{k,i}(t)}{1 - \xi_{k,i}(t)}\right), \tag{18}$$

where $\xi_{k,i} = e_{k,i} / \rho_{k,i}$ and $i = 1, 2, \cdots, n$ are the normalized errors. The $i+1$-th virtual control signals $v_{k,i+1}$, $k = 1, \cdots, N$, and $i = 1, \cdots, n-1$ are designed as

$$v_{k,i+1} = -K_{k,i} r_{k,i}, \tag{19}$$

where $K_{k,i}$ is a positive control parameter. At this stage, the actual tracking control signal u_k is designed as

$$u_k = -K_{k,n} r_{k,n}, \tag{20}$$

where $K_{k,n}$ is a positive control parameter.

Remark 8. It is worth pointing out that the output performance function $\rho_{k,i}(t)$ is applied to limit the error $e_{k,i}(t)$ within the imposed time-varying constraints. Given any initial condition, the constants $\rho_{k,i}^0$, $i = 1, \cdots, n$ is selected satisfying $\rho_{k,i}^0 > |e_{k,i}(0)|$, and $\rho_{k,i}^\infty$ represents the maximum allowable value of the steady-state $e_{k,i}(t)$, which can be assigned to an arbitrarily small value. Hence, the convergence of $e_{k,i}(t)$ to a predefined set of arbitrary small residuals is realized. Furthermore, the rate of $\rho_{k,i}(t)$ decline is influenced by $l_{k,i}$ and results in the lower bound of the required rate of $e_{k,i}(t)$ convergence. Therefore, $e_{k,i}(t)$ is restricted to a preassigned boundary by using the performance function.

Remark 9. Under transient and steady state responses, for the construction of (17), the proposed control scheme (19) and (20) merely made up of nonlinear transformation error surfaces and design constants can be designed to preallocate the tracking performance boundary.

3.3. Stability and Performance Analysis

Theorem 10. *Consider system (4) obeying Assumption 1 and Assumption 2 controlled by the virtual control signals (19) and the proposed distributed controller (20), all the signals in the closed-loop system are globally bounded. Then, we have the following properties:*

(1) The normalized error $\xi_{k,i}(t)$, $k = 1, \cdots, N$, and $i = 1, \cdots, n$ satisfies $|\xi_{k,i}(t)| < 1$, which can be guaranteed by prespecified tracking performance

(2) The outputs of each agent eventually satisfy $\lim_{t \to +\infty} |y_k(t) - y_d(t)| < \rho_{k,1}^\infty$, where $k = 1, \cdots, N$

Proof. From the definition of the errors, the states $x_1, \cdots, x_n$ can be rewritten as

$$\begin{aligned} x_{k,1} &= e_{k,1} + q_{k,1}, \\ x_{k,i} &= e_{k,i} + \nu_{k,i}, \; i = 2, \cdots, n. \end{aligned} \tag{21}$$

Let $\xi_i(t) = [\xi_{1,i}(t), \cdots, \xi_{N,i}(t)]^T \in \mathbb{R}^N$, from the definition of $\xi_i(t)$, we can get that

$$\dot{\xi}_{k,1} = \frac{f_{k,1}(t, \bar{x}_{k,1}) + g_{k,1}(t, \bar{x}_{k,1}) x_{k,2}^{p_{k,1}} - q_{k,2} - \xi_{k,1}\dot{\rho}_{k,1}}{\rho_{k,1}}, \tag{22}$$

$$\dot{\xi}_{k,i} = \frac{f_{k,i}(t, \bar{x}_{k,i}) + g_{k,i}(t, \bar{x}_{k,i}) x_{k,i+1}^{p_{k,i}} - \dot{\nu}_{k,i} - \xi_{k,i}\dot{\rho}_{k,i}}{\rho_{k,i}}, \; i = 2, \cdots, n-1, \tag{23}$$

$$\dot{\xi}_{k,n} = \frac{f_{k,n}(t, \bar{x}_{k,n}) + g_{k,n}(t, \bar{x}_{k,n})(h_k(t)u_k + d_k(t))^{p_{k,n}} - \dot{\nu}_{k,n} - \xi_{k,n}\dot{\rho}_{k,n}}{\rho_n}. \tag{24}$$

By denoting $r_i(t) = [r_{1,i}(t), \cdots, r_{N,i}(t)]^T \in \mathbb{R}^N$, $i = 1, \cdots, n$, the time derivative of $r_i(t)$ can be given by

$$\dot{r}_{k,1} = \mu_{k,1}\left(f_{k,1}(t, \bar{x}_{k,1}) + g_{k,1}(t, \bar{x}_{k,1}) x_{k,2}^{p_{k,1}} - q_{k,2} - \xi_{k,1}\dot{\rho}_{k,1}\right), \tag{25}$$

$$\dot{r}_{k,i} = \mu_{k,i}\left(f_{k,i}(t, \bar{x}_{k,i}) + g_{k,i}(t, \bar{x}_{k,i}) x_{k,i+1}^{p_{k,i}} - \dot{\nu}_{k,i} - \xi_{k,i}\dot{\rho}_{k,i}\right), \; i = 2, \cdots, n-1, \tag{26}$$

$$\dot{r}_{k,n} = \mu_{k,n}\left(f_{k,n}(t, \bar{x}_{k,n}) + g_{k,n}(t, \bar{x}_{k,n})(h_k(t)u_k + d_k(t))^{p_{k,n}} - \dot{\nu}_{k,n} - \xi_{k,n}\dot{\rho}_{k,n}\right), \tag{27}$$

where $\mu_{k,i} = 2/(\rho_{k,i}(1 - \xi_{k,i}^2)) \in \mathbb{R}$.

The performance functions $\rho_{k,i}(t)$ have been chosen to meet requirements as $\rho_{k,i}^0 > |e_{k,i}(0)|$, which equals to $\bar{\xi}(0) \in \Upsilon$ where $\Upsilon = \Upsilon_1 \times \cdots \times \Upsilon_n$ an open set with $\Upsilon_i = (-1, 1)$, $i = 1, \cdots, n$. Additionally, the fact that from (17), the desired trajectory y_d and the performance functions $\rho_{k,i}(t)$ are bounded and continuously differentiable with respect to time. The intermediate control signals $\nu_{k,i}$, $i = 2, \cdots, n$, and the control law $u_{k,i}$ are smooth over the set Υ. It is deduced that $\dot{\xi}_k(t)$ is bounded and piecewise continuous in t and locally Lipschitz on $\xi_k(t)$ over Υ. According to Theorem 54 of [33], the conditions on $\dot{\xi}_k(t)$ ensure the existence and uniqueness of a maximal solution $\xi_k(t)$ of (22)–(24) over the set Υ, for $\forall t \in [0, \tau_{\max})$, $k = 1, \cdots, N$, $i = 1, \cdots, n$ such that $\xi_k(t) \in \Upsilon$, $\forall t \in [0, \tau_{\max})$ or equivalently that for $\forall t \in [0, \tau_{\max})$, the following formula holds

$$\xi_{k,i}(t) \in (-1, 1). \tag{28}$$

Since $r_{k,i}$ is well established. □

Next, $\tau_{\max} = +\infty$ will be proved by looking for a contradiction. It is supposed that $\tau_{\max} < +\infty$, thus, the following analysis is performed. And a systematic procedure for the proof of the aforementioned statements is given below for $t \in [0, \tau_{\max})$.

Step 1. From (17) and (28), for any $t \in [0, \tau_{\max})$, $x_{k,1}(t)$ is bounded as

$$|x_{k,1}(t)| = |\xi_{k,1}(t)\rho_{k,1}(t) + q_{k,1}(t)| \le \rho_{k,i}^0 + \bar{q}_{k,1}, \tag{29}$$

where $\bar{q}_{k,1} > 0$ is a constant such that $|q_{k,1}| < \bar{q}_{k,1}$. Moreover, the boundedness of $x_{k,1}$ results in the boundedness of the functions $f_{k,1}(t, x_{k,1})$ as

$$|f_{k,1}(t, x_{k,1})| \le \beta_{k,1}(x_{k,1}(t)), \tag{30}$$

where $\beta_{k,1}(x_{k,1})$ is a positive C^1 nonlinear function.

By denoting $r_i(t) = [r_{1,i}(t), \cdots, r_{N,i}(t)]^T \in \mathbb{R}^N$, establish the first Lyapunov function candidate as

$$V_1 = \frac{1}{2} r_1^T r_1. \tag{31}$$

Substituting (18) and (22), the time derivative of V_1 is derived as follows

$$\dot{V}_1 = \sum_{k=1}^{N} r_{k,1}\mu_{k,1}\left(f_{k,1}(t, x_{k,1}) + g_{k,1}(t, x_{k,1}) x_{k,2}^{p_1} - q_{k,2} - \dot{\rho}_{k,1}\xi_{k,1}\right). \tag{32}$$

Using (30) and yields

$$\sum_{k=1}^{N}\left(f_{k,1}(x_{k,1}) - q_{k,2} - \xi_{k,1}\dot{\rho}_{k,1}\right) \le \sum_{k=1}^{N} \breve{\iota}_{k,1} \le \sum_{k=1}^{N} C_{k,1}, \tag{33}$$

where $\breve{\iota}_{k,1} \triangleq \beta_{k,1}(x_{k,1}) + |q_{k,2}| + |\varsigma_{k,1}\dot{\rho}_{k,1}|$ and $C_{k,1}$ is a positive constant.

Applying Lemma 3 to the terms $r_{k,1}\mu_{k,1}g_{k,1}(t, x_{k,1})x_{k,2}^{p_1}$, using $e_{k,2} = x_{k,2} - \nu_{k,2}$ and $e_{k,2} = \xi_{k,2}\rho_{k,2}$, one has

$$\begin{aligned} & r_{k,1}\mu_{k,1}g_{k,1}(t, x_{k,1})\left(\xi_{k,2}\rho_{k,2} + \nu_{k,2}\right)^{p_{k,1}} \\ & \quad \le -\frac{K_{k,1}^{p_{k,1}}\underline{g}_{k,1}}{2^{p_{k,1}-1}}\mu_{k,1}r_{k,1}^{p_{k,1}+1} + \mu_{k,1}r_{k,1}\bar{g}_{k,1}\left(\xi_{k,2}\rho_{k,2}\right)^{p_{k,1}}, \end{aligned} \tag{34}$$

where $\underline{g}_{k,1}$ and $\bar{g}_{k,1}$ are both positive constants satisfying $\underline{g}_{k,1} \le g_{k,1}(t, x_{k,1}) \le \bar{g}_{k,1}$.

Combining (33) and (34), we obtain

$$\dot{V}_1 = \sum_{k=1}^{N} -\bar{\kappa}_{k,1}\mu_{k,1}r_{k,1}^{p_{k,1}+1} + \left(\bar{g}_{k,1}\left(\rho_{k,2}^0\right)^{p_{k,1}} + C_{k,1}\right)\mu_{k,1}|r_{k,1}|, \tag{35}$$

where $\bar{\kappa}_{k,1} = K_{k,1}^{p_{k,1}}\underline{g}_{k,1}/2^{p_{k,1}-1}$.

Applying Lemma 4 to the terms $\bar{\kappa}_{k,1}\mu_{k,1}r_{k,1}^{p_{k,1}+1}$, one has

$$\bar{\kappa}_{k,1}\mu_{k,1}|r_{k,1}| \le \frac{\bar{\kappa}_{k,1}\mu_{k,1}}{p_{k,1}+1}r_{k,1}^{p_{k,1}+1} + \frac{p_{k,1}}{p_{k,1}+1}\bar{\kappa}_{k,1}\mu_{k,1}. \tag{36}$$

Therefore, (35) becomes

$$\dot{V}_1 = \sum_{k=1}^{N}\mu_{k,1}\left(-\tilde{\kappa}_{k,1}|r_{k,1}| + \iota_{k,1}\right), \tag{37}$$

where $\tilde{\kappa}_{k,1} = \bar{\kappa}_{k,1}(p_{k,1}+1) - \bar{g}_{k,1}(\rho_{k,2}^0)^{p_{k,1}} - C_{k,1}$, $\iota_{k,1} = p_{k,1}\bar{\kappa}_{k,1}$. From (37), for all $t \in [0, \tau_{\max})$, it follows that $\dot{V}_1$ is negative when $|r_{k,1}| \ge \iota_{k,1}/\widehat{\kappa}_1$, where $\widehat{\kappa}_1 = \min_{0\le k\le N, k\in N^+}\{\tilde{\kappa}_{k,1}\}$ and subsequently that $|r_{k,1}(t)| < \bar{r}_{k,1} \le \bar{r}_1 \triangleq \max_{0\le k\le N, k\in N^+}\{\iota_{k,1}/\widehat{\kappa}_1\}$, which implies that the normalized error is bounded as

$$-1 < \frac{e^{-\bar{r}_1}-1}{e^{-\bar{r}_1}+1} = \xi_{k,1\text{low}} < \xi_{k,1}(t) < \xi_{k,1\text{upper}} = \frac{e^{\bar{r}_1}-1}{e^{\bar{r}_1}+1} < 1, \tag{38}$$

for $k = 1, \cdots, N$. According to (19), for all $t \in [0, \tau_{\max})$, the boundedness of r_1 results in the boundedness of $v_2(t)$. Additionally, from $\xi_{k,i} = e_{k,i}/\rho_{k,i}$, we conclude that

$$-\rho_{k,1}(t) < \frac{e^{-\bar{r}_1}-1}{e^{-\bar{r}_1}+1}\rho_{k,1}(t) \le e_{k,1}(t) \le \frac{e^{\bar{r}_1}-1}{e^{\bar{r}_1}+1}\rho_{k,1}(t) < \rho_{k,1}(t). \tag{39}$$

Step $i (i = 2, \cdots, n-1)$: construct the $i-$th Lyapunov function as

$$V_i = \frac{1}{2}r_i^T r_i. \tag{40}$$

Differentiating along (40) with respect to time, using (26), yields

$$\dot{V}_i = \sum_{k=1}^{N} r_{k,i}\mu_{k,i}\left(f_{k,i}(t,\bar{x}_{k,i}) + g_{k,i}(t,\bar{x}_{k,i})x_{k,i+1}^{p_{k,i}} - \dot{v}_{k,i} - \dot{\rho}_{k,i}\xi_{k,i}\right). \tag{41}$$

According to the boundedness of $v_i(t)$ in the last step, using $e_{k,i} = x_{k,i} - v_{k,i}$, $e_{k,i} = \xi_{k,i}\rho_{k,i}$, and (28), $x_{k,i}(t)$ is bounded as $|x_{k,i}(t)| = |\xi_{k,i}(t)\rho_{k,i}(t) + v_{k,i}(t)| \le \rho_{k,i}^0 + |v_{k,i}|$, $k = 1, \cdots, N$, and $i = 1, \cdots, n$. Furthermore, the boundedness of $\bar{x}_{k,i}(t)$ results in the boundedness of $f_{k,i}$. From (38), for all $t \in [0, \tau_{\max})$, $\mu_{k,i-1} = 2/(\rho_{k,i-1}(1-\xi_{k,i-1}^2)) \in \mathbb{R}$ is also bounded. Moreover, $\dot{v}_i(t)$ is bounded. Similar to (30) and (33), there

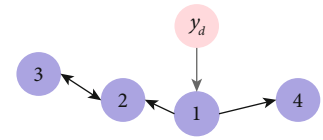

Figure 2: Communication topology for 4 subsystems.

is a C^1 nonlinear function $\breve{\iota}_{k,i}$, and we have

$$\begin{aligned}\dot{V}_i &\le \sum_{k=1}^{N} r_{k,i}\mu_{k,i}\left(g_{k,i}(t,\bar{x}_{k,i})x_{k,i+1}^{p_{k,i}} + \breve{\iota}_{k,i}\right)\\ &\le \sum_{k=1}^{N} r_{k,i}\mu_{k,i}\left(g_{k,i}(t,\bar{x}_{k,i})x_{k,i+1}^{p_{k,i}} + C_{k,i}\right),\end{aligned} \tag{42}$$

where $\breve{\iota}_{k,i} \triangleq |f_{k,i}(t,\bar{x}_{k,i})| + |\dot{v}_{k,i}| + |\xi_{k,i}\dot{\rho}_{k,i}|$ and $C_{k,i}$ is a positive constant.

Applying Lemma 3 to the terms $g_{k,i}(t,\bar{x}_{k,i})x_{k,i+1}^{p_{k,i}}$, using $e_{k,i+1} = \xi_{k,i+1}\rho_{k,i+1}$, (42) becomes

$$\dot{V}_i \le \sum_{k=1}^{N} -\bar{\kappa}_{k,i}\mu_{k,i}r_{k,i}^{p_{k,i}+1} + \left(\breve{\kappa}_{k,i} + C_{k,i}\right)\mu_{k,i}|r_{k,i}|, \tag{43}$$

where $\bar{\kappa}_{k,1} = K_{k,1}^{p_{k,1}}\underline{g}_{k,1}/2^{p_{k,1}-1}$, $\breve{\kappa}_{k,i} = \bar{g}_{k,i}(\rho_{k,i}^0)^{p_{k,i}}$, $\underline{g}_{k,i} > 0$, and $\bar{g}_{k,i} > 0$ are both constants satisfying $\underline{g}_{k,i} \le g_{k,i}(t,\bar{x}_{k,i}) \le \bar{g}_{k,i}$.

Then, applying Lemma 4 to the terms $\bar{\kappa}_{k,i}\mu_{k,i}r_{k,i}^{p_{k,i}+1}$ yields

$$\bar{\kappa}_{k,i}\mu_{k,i}|r_{k,i}| \le \mu_{k,i}\frac{\bar{\kappa}_{k,i}}{p_{k,i}+1}r_{k,i}^{p_{k,i}+1} + \mu_{k,i}\frac{p_{k,i}}{p_{k,i}+1}\bar{\kappa}_{k,i}. \tag{44}$$

Thus, (43) becomes

$$\dot{V}_i = \sum_{k=1}^{N}\mu_{k,i}\left(-\tilde{\kappa}_{k,i}|r_{k,i}| + \iota_{k,i}\right), \tag{45}$$

where $\tilde{\kappa}_{k,i} = \bar{\kappa}_{k,i}(p_{k,i}+1) - \breve{\kappa}_{k,i} - C_{k,i}$, $\iota_{k,i} = p_{k,i}\bar{\kappa}_{k,i}$. From (45), we conclude that $\dot{V}_i < 0$ when $|r_{k,i}| \ge \iota_{k,i}/\widehat{\kappa}_i$, where $\widehat{\kappa}_i = \min_{0\le k\le N, k\in N^+}\{\tilde{\kappa}_{k,i}\}$ and subsequently that $|r_{k,i}(t)| < \bar{r}_{k,i} \le \bar{r}_i \triangleq \max_{0\le k\le N, k\in N^+}\{\iota_{k,i}/\widehat{\kappa}_i\}$ for all $t \in [0, \tau_{\max})$. Additionally, for all $t \in [0, \tau_{\max})$ by using (18), we get

$$-1 < \frac{e^{-\bar{r}_i}-1}{e^{-\bar{r}_i}+1} = \xi_{i,\text{low}} < \xi_{k,i}(t) < \xi_{i,\text{upper}} = \frac{e^{\bar{r}_i}-1}{e^{\bar{r}_i}+1} < 1, \tag{46}$$

From $\xi_{k,i} = e_{k,i}/\rho_{k,i}$, (46) implies that

$$-\rho_{k,i}(t) < \frac{e^{-\bar{r}_{i1}}-1}{e^{-\bar{r}_i}+1}\rho_{k,i}(t) \le e_{k,i}(t) \le \frac{e^{\bar{r}_i}-1}{e^{\bar{r}_i}+1}\rho_{k,i}(t) < \rho_{k,i}(t). \tag{47}$$

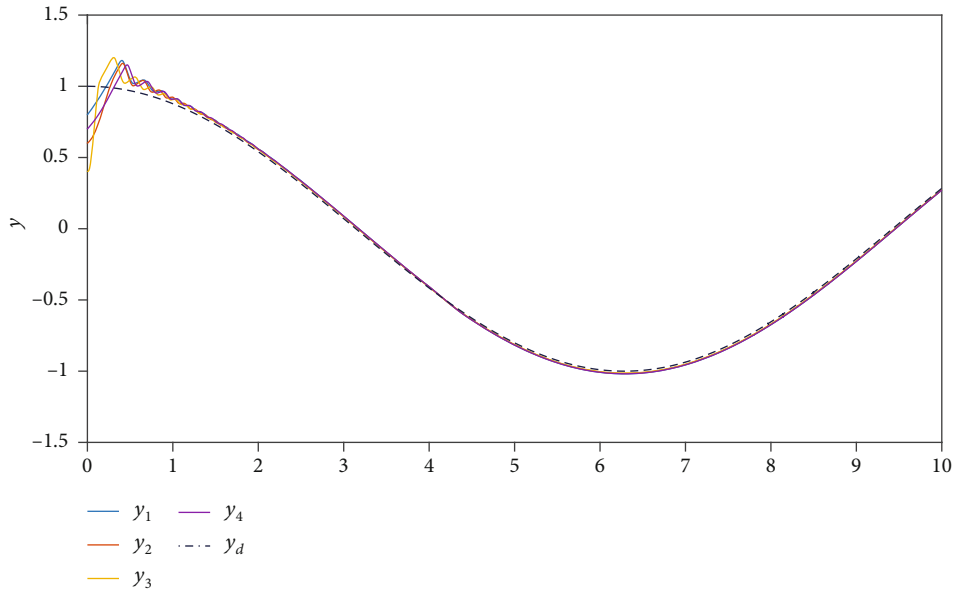

Figure 3: The output tracking performance y_k and y_d.

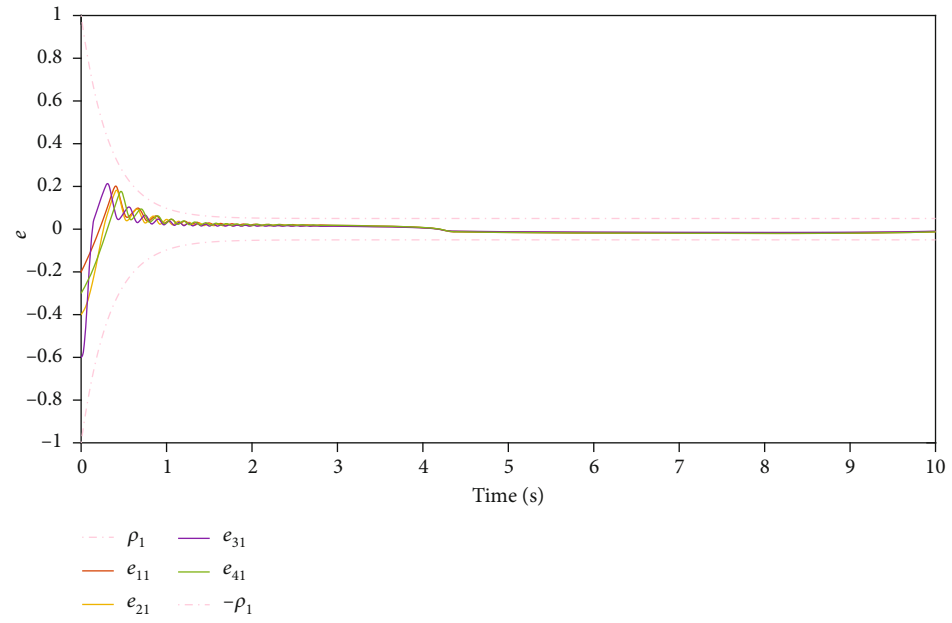

Figure 4: The error $e_{k,1}$ of the closed-loop system.

In addition, according to (19), the boundedness of r_i results in the boundedness of $v_{i+1}(t)$, $i = 2, \cdots, n-1$ for all $t \in [0, \tau_{\max})$.

Step n: construct the final Lyapunov function as

$$V_n = \frac{1}{2} r_n^T r_n. \tag{48}$$

Differentiating along (48) with respect to time and invoking (18) and (24), one has

$$\dot{V}_n = \sum_{k=1}^{N} r_{k,n}\mu_{k,n}\left(f_{k,n}(t, \bar{x}_{k,n}) - \dot{v}_{k,n} - \xi_{k,n}\dot{\rho}_{k,n} + g_{k,n}(t, \bar{x}_{k,n})(h_k(t)u_k + d_k(t))^{p_{k,n}}\right). \tag{49}$$

It can be deduced that for all $t \in [0, \tau_{\max})$, $\mu_{k,n-1}$ is bounded from (46). Based on the boundedness of $v_{k,n}(t)$ in the $n-1$ step. Additionally, from (17), (28), it is obviously

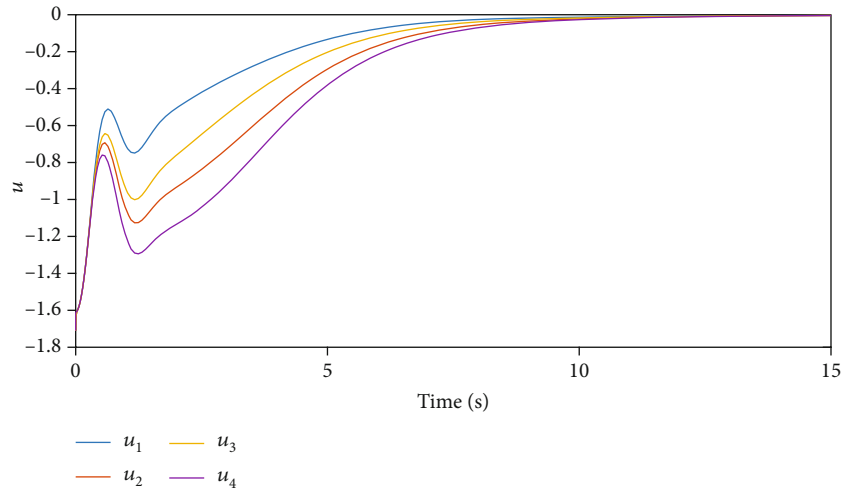

Figure 5: Control input u with deadzone.

that $x_{k,n}(t)$ is bounded as $|x_{k,n}(t)| = |\xi_{k,n}(t)\rho_{k,n}(t) + \nu_{k,n}(t)| \le \rho_{k,n}^0 + |\nu_{k,n}|$ for all $t \in [0, \tau_{\max})$. From (19), $\dot{\nu}_{k,n}$ is also bounded. Then, the boundedness of $\bar{x}_{k,n}$ results in the boundedness of $f_{k,n-1}(t, \bar{x}_{k,n-1})$. Therefore, there is a constant $C_{k,n} > 0$ satisfying $|f_{k,n}(t, \bar{x}_{k,n})| + |\dot{\nu}_{k,n}| + |\xi_{k,n}\dot{\rho}_{k,n}| \triangleq \breve{\iota}_{k,n} \le C_{k,n}$, such that

$$\dot{V}_{k,n} \le \sum_{k=1}^{N} \mu_{k,n} r_{k,n} g_{k,n}(t, \bar{x}_{k,n})(h_k(t)u_k + d_k(t))^{p_{k,n}} + \mu_{k,n}|r_{k,n}|C_{k,n}. \tag{50}$$

Under Assumption 2 and Lemma 3, invoking (20) and the previous analysis yields

$$\begin{aligned} &\mu_{k,n} g_{k,n}(t, \bar{x}_{k,n}) r_{k,n}(h_k(t)u_k + d_k(t))^{p_{k,n}} \\ &\quad = \mu_{k,n} g_{k,n} r_{k,n}\left((-K_{k,n}h_k r_{k,n} + d_k)^{p_{k,n}} - d_k^{p_{k,n}} + d_k^{p_{k,n}}\right) \\ &\quad \le -\frac{\mu_{k,n} K_{k,n}^{p_{k,n}} |g_{k,n}|}{2^{p_{k,n}-1}} \underline{h}_k^{p_{k,n}} r_{k,n}^{p_{k,n}+1} + \mu_{k,n} g_{k,n} r_{k,n} \bar{d}_k^{p_{k,n}}, \end{aligned} \tag{51}$$

where $\underline{h}_k$ is an unknown positive constant satisfying $\underline{h}_k \le \breve{h}_k(u) \le |h_k(u)|$, with an unknown positive continuous function $\breve{h}_k(u)$. Invoking (51) and Assumption 2, we have

$$\dot{V}_n \le \sum_{k=1}^{N} \mu_{k,n}\left(-\frac{K_n^{p_{k,n}} \underline{g}_{k,n}}{2^{p_{k,n}-1}} \underline{h}_k^{p_{k,n}} r_{k,n}^{p_{k,n}+1} + |r_{k,n}| \bar{\iota}_{k,n}\right), \tag{52}$$

where $\bar{\iota}_{k,n} = C_{k,n} + \bar{g}_{k,n}\bar{d}_k^{p_{k,n}}$ with an unknown positive constant $\bar{d}_k$ satisfying $\bar{d}_k \le \bar{d}_k(u)$, $\underline{g}_{k,n}$ and $\bar{g}_{k,n}$ are both positive constants satisfying $\underline{g}_{k,n} \le g_{k,n}(t, \bar{x}_{k,n}) \le \bar{g}_{k,n}$.

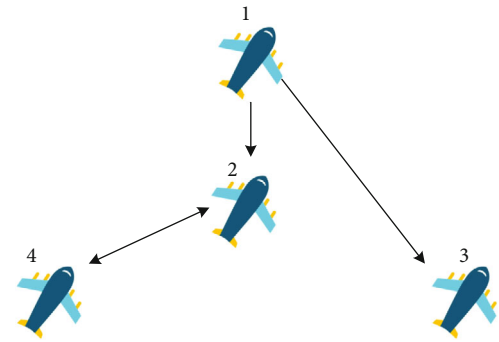

Figure 6: Communication topology for 4 fighters.

Substituting (20) into the third term of (52) yields

$$\dot{V}_n \le \sum_{k=1}^{N} -\frac{K_n^{p_{k,n}} \underline{g}_{k,n} \underline{h}_k^{p_{k,n}}}{2^{p_{k,n}-1}} \mu_{k,n} r_{k,n}^{p_{k,n}+1} + \mu_{k,n} \bar{\iota}_{k,n} |r_{k,n}|. \tag{53}$$

Applying Lemma 4 to the term $\underline{g}_{k,n}\underline{h}_k^{p_{k,n}}\mu_{k,n} r_{k,n}^{p_{k,n}+1}$, we obtain

$$\underline{g}_{k,n}\underline{h}_k^{p_n}\mu_{k,n}|r_{k,n}| \le \frac{\underline{g}_{k,n}\underline{h}_k^{p_n}\mu_{k,n}}{p_{k,n}+1} r_{k,n}^{p_n+1} + \frac{p_{k,n}}{p_{k,n}+1}\underline{g}_{k,n}\underline{h}_k^{p_n}\mu_{k,n}. \tag{54}$$

Thus, (53) becomes

$$\dot{V}_n \le \sum_{k=1}^{N} \mu_{k,n}\left(-\tilde{\kappa}_{k,n}|r_{k,n}| + \iota_{k,n}\right), \tag{55}$$

where $\tilde{\kappa}_{k,n} = K_n^{p_{k,n}} \underline{g}_{k,n} \underline{h}_k^{p_{k,n}} (p_{k,n}+1)/2^{p_{k,n}-1} - \bar{\iota}_{k,n}$ and $\iota_{k,n} = K_n^{p_{k,n}} p_{k,n} \underline{g}_{k,n} \underline{h}_k^{p_{k,n}} / 2^{p_{k,n}-1}$. Then, where $\dot{V}_n$ is negative when $|r_{k,n}(t)| \ge \iota_{k,n}/\bar{\kappa}_n$, where $\bar{\kappa}_n = \min_{0 \le k \le N, k \in N^+} \{\tilde{\kappa}_{k,n}\}$, we obtain $|r_{k,n}(t)| < \bar{r}_{k,n} \le \bar{r}_n \triangleq \max_{0 \le k \le N, k \in N^+} \{\iota_{k,n}/\bar{\kappa}_n\}$ for all $t \in [0, \tau_{\max})$.

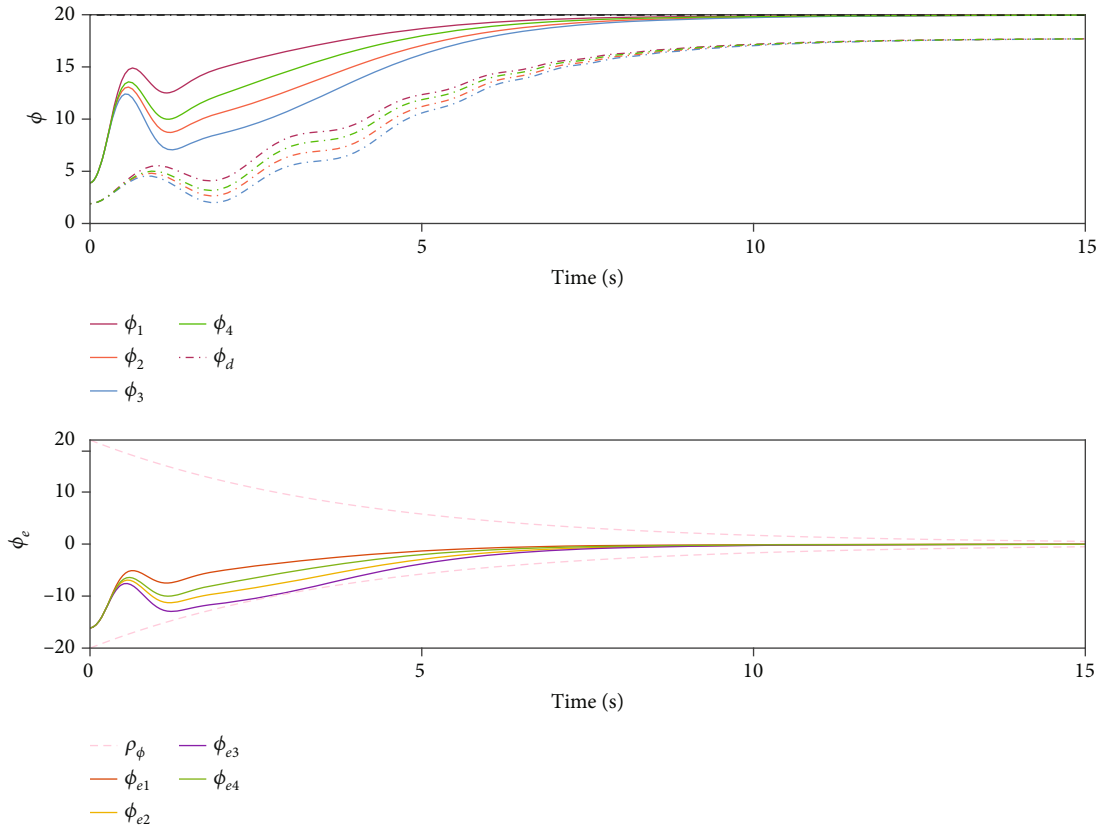

Figure 7: Roll angle ϕ.

Invoking (18), for $k = 1, \cdots, N$, we get

$$-1 < \frac{e^{-\bar{r}_n} - 1}{e^{-\bar{r}_n} + 1} = \xi_{n,\text{low}} < \xi_{k,n}(t) < \xi_{n,\text{upper}} = \frac{e^{\bar{r}_n} - 1}{e^{\bar{r}_n} + 1} < 1. \quad (56)$$

From $\xi_{k,n} = e_{k,n}/\rho_{k,n}$, (56) implies that

$$-\rho_{k,n}(t) < \frac{e^{-\bar{r}_{n1}} - 1}{e^{-\bar{r}_{n1}} + 1}\rho_{k,n}(t) \le e_{k,n}(t) \le \frac{e^{\bar{r}_n} - 1}{e^{\bar{r}_n} + 1}\rho_{k,n}(t) < \rho_{k,n}(t). \quad (57)$$

As a result, due to (20), the control signal $u_{k,n}(t)$ is bounded from the boundedness of $r_{k,n}(t)$. Moreover, for all $t \in [0, \tau_{\max})$, (38), (46), and (56) imply that $\xi_{k,i}(t) \in \Upsilon_\xi \subset \Upsilon$, where the set $\Upsilon_\xi = (\xi_{i,\text{low}}, \xi_{i,\text{upper}}) \times \cdots \times (\xi_{n,\text{low}}, \xi_{n,\text{upper}})$ is nonempty and compact. Thus, it is an obvious contradiction to assume that $\tau_{\max} < +\infty$ determines the existence of a temporal instant $t_\xi \in [0, \tau_{\max})$, which means that $e_{k,i}(t_\xi) \notin \Upsilon_\xi$. Therefore, $\tau_{\max} = +\infty$. Finally, from (39), (47), and (57), we can draw the conclusion that $|e_{k,i}(t)| < \rho_{k,i}(t)$ for all $t \ge 0$. Based on the exponential decay property of $\rho_{k,i}$, the following inequality holds $\lim_{t\longrightarrow\infty}|e_{k,i}| < \rho_{k,i}^{\infty}$, $k = 1, \cdots, N$, and $i = 1, \cdots, n$. Then, in view of (15), we have $|y_k(t) - y_d(t)| = |y_k(t) - q_{k,1}(t) + q_{k,1}(t) - y_d(t)| \le |e_{k,1}(t)| + |q_{k,1}(t) - y_d(t)|$. Based on Theorem 7, it can be derived that

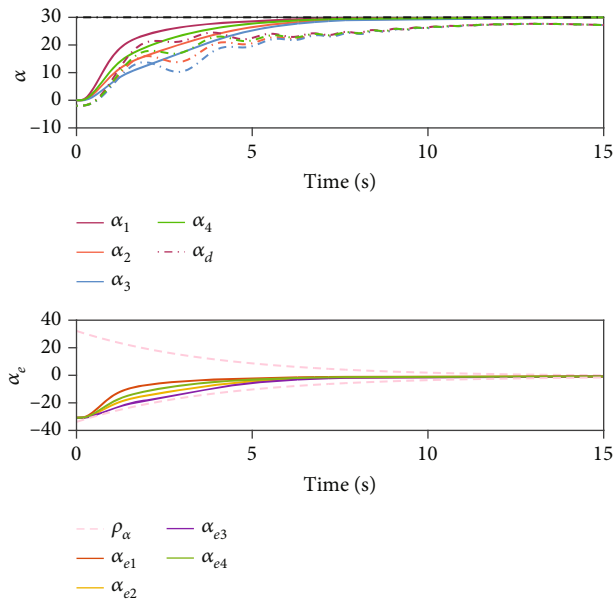

Figure 8: Attack angle α.

$$\lim_{t\longrightarrow+\infty}|y_k(t) - y_d(t)| < \rho_{k,1}^{\infty}. \quad (58)$$

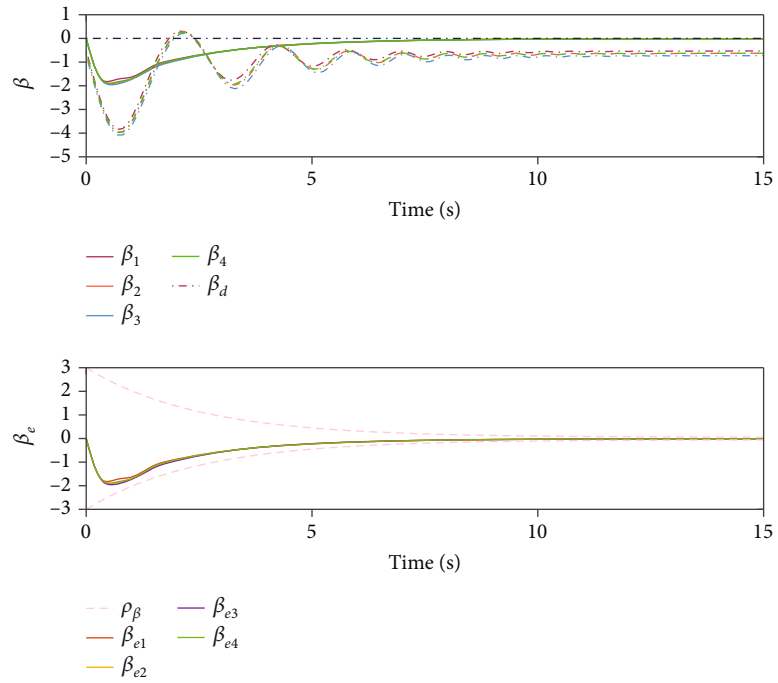

Figure 9: Sideslip angle β.

In the Lyapunov sense, $e_{k,i}(t)$ is kept within the preassigned boundary of transient and steady state range, and this is the end of the proof.

Remark 11. From Theorem 10, it should be noticed that this memoryless control tracker is recursively constructed by virtue of the specified performance design method, and the transient and steady state performance boundaries of $e_{k,i}$ are up to the performance functions $\rho_{k,i}$.

4. Simulation Study

A numerical simulation study and a practical simulation study are presented in this section to give evidence of the efficacy and advantage of the constructed control design.

Example 1. Consider the uncertain MAS with unknown high powers and input deadzone with a communication topology depicted in Figure 2 as follows

$$\begin{aligned}
\dot{x}_{k,1} &= f_{k,1}(t, x_{k,1}) + g_{k,1}(t, x_{k,1}) x_{k,2}^{p_{k,1}}, \\
\dot{x}_{k,2} &= f_{k,2}(t, \bar{x}_{k,2}) + g_{k,2}(t, \bar{x}_{k,2}) x_{k,3}^{p_{k,2}}, \\
\dot{x}_{k,3} &= f_{k,3}(t, \bar{x}_{k,3}) + g_{k,3}(t, \bar{x}_{k,3}) (h_k(t) u_k + d_k(t, u))^{p_{k,3}}, \\
y_k &= x_{k,1}, \quad k = 1, \cdots, 4,
\end{aligned} \tag{59}$$

where $p_{k,1} = p_{k,2} = p_{k,3} = 3$, $g_{k,1} = 0.8 + 0.5x_1^2$, $g_{k,2} = 1 + 0.4 \sin(x_3)$, $g_{k,3} = 1$, $f_{k,1} = \sin(x_{k,1})$, $f_{k,2} = x_{k,3} \cos(x_{k,2})$, $f_{k,3} = x_{k,3} \sin^2(x_{k,2})$, and $k = 1, \cdots, 4$. The desired signal is $y_d = \cos(0.5t)$. The initial conditions are selected as $x_{k,1}^0 = 0.5$, $x_{k,2}^0 = 0$, $x_{k,3}^0 = 0$, and $k = 1, \cdots, 4$.

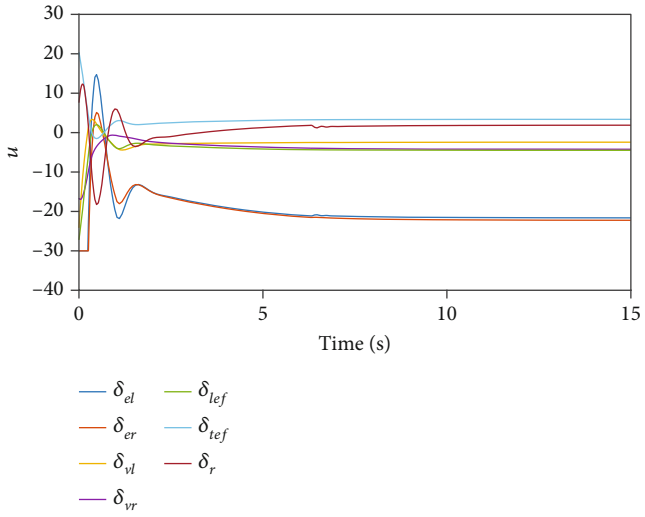

Figure 10: The responses of actuator of fighter 1.

The proposed tracking control scheme with prescribed performance is established as follows.

$$\begin{aligned}
v_{k,2} &= -K_{k,1} r_{k,1}, \\
v_{k,3} &= -K_{k,2} r_{k,2}, \\
u_k &= -K_{k,3} r_{k,3},
\end{aligned} \tag{60}$$

where the control parameters are $K_{k,1} = 2.8$, $K_{k,2} = 5$, $K_{k,3} = 18$, and $k = 1, \cdots, 4$.

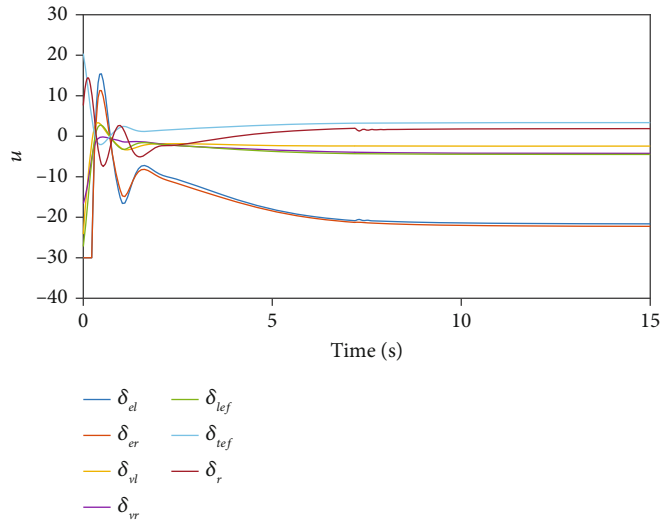

Figure 11: The responses of actuator of fighter 2.

From $e_1(0) = y(0) - y_d(0) = -0.5$, $e_2(0) = x_2(0) - v_2(0)$, and $e_3(0) = x_3(0) - v_3(0)$, set $\rho_0 = [\rho_{1,0}, \rho_{2,0}, \rho_{3,0}]^T = [3.5, 4.5, 2]^T$ such that $\rho_0 > |e_0|$. For the preselected bound of e_1, e_2, and e_3, design $\rho_1 = (3.5 - 0.35)e^{-2t} + 0.35$, $\rho_2 = (4.5 - 0.30)e^{-3t} + 0.30$, and $\rho_3 = (2 - 0.5)e^{-t} + 0.5$.

In addition, to emphasize the capacity of the proposed controller to deal with the deadzone with a $u - D(u)$ characteristic in the presence of nominal deviation from linear slopes, we consider the deadzone function (2) where $h_l(t) = 0.80 + 0.2 \sin(t)$, $h_r(t) = 0.75 + 0.2 \cos(t)$, $b_l = -0.7$, and $b_r = 0.5$.

As expected, from these simulation results shown in Figures 3–5, it is indicated that the desired tracking performance can be realized, and all the closed loop signals are bounded under the proposed distributed controller.

Example 2. Consider the dynamics of four practical high maneuverer fighters with input deadzone as follows [34], and for simplicity, the subscripts of the following aerodynamic variables are omitted (i.e., $\phi_k = \phi, \alpha_k = \alpha, \beta_k = \beta$ and so on).

$$\begin{aligned}
\dot{x}_{k,1} &= f_{k,1}(t, x_{k,1}) + g_{k,1}(t, x_{k,1}) x_{k,2}^{p_{k,1}}, \\
\dot{x}_{k,2} &= f_{k,2}(t, \bar{x}_{k,2}) + g_{k,2}(t, \bar{x}_{k,2}) x_{k,3}^{p_{k,2}}, \\
\dot{x}_{k,3} &= f_{k,3}(t, \bar{x}_{k,3}) + g_{k,3}(t, \bar{x}_{k,3}) (h_k(t) u_k + d_k(t, u))^{p_{k,3}}, \\
y_k &= x_{k,1}, \quad k = 1, \cdots, 4,
\end{aligned} \tag{61}$$

with

$$f_{k,1}(t, x_{k,1}) = \begin{bmatrix} q \tan\theta \sin\phi + r \tan\theta \cos\phi \\ p\beta + z_0 \Delta\alpha + (g_0/V)(\cos\theta \cos\phi - \cos\theta_0) \\ y_\beta \beta + p(\sin\alpha_0 + \Delta\alpha) + (g_0/V) \cos\theta \sin\phi \end{bmatrix}, \tag{62}$$

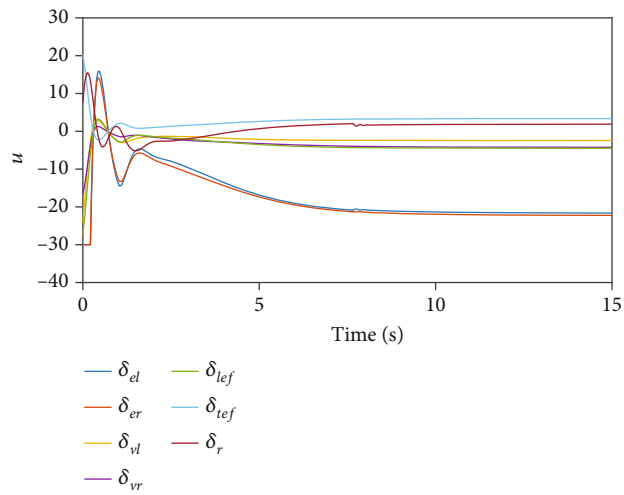

Figure 12: The responses of actuator of fighter 3.

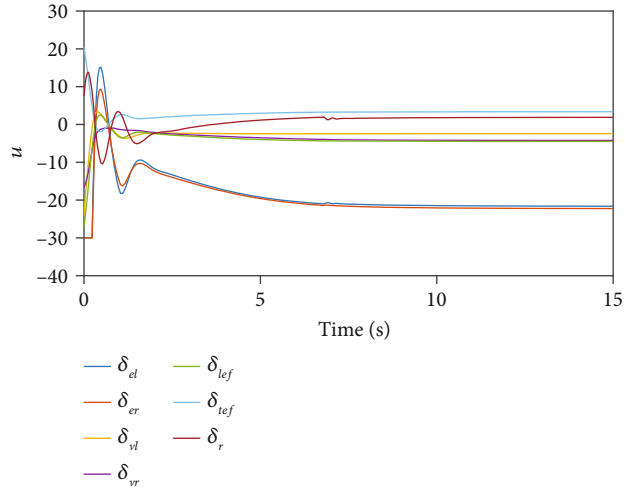

Figure 13: The responses of actuator of fighter 4.

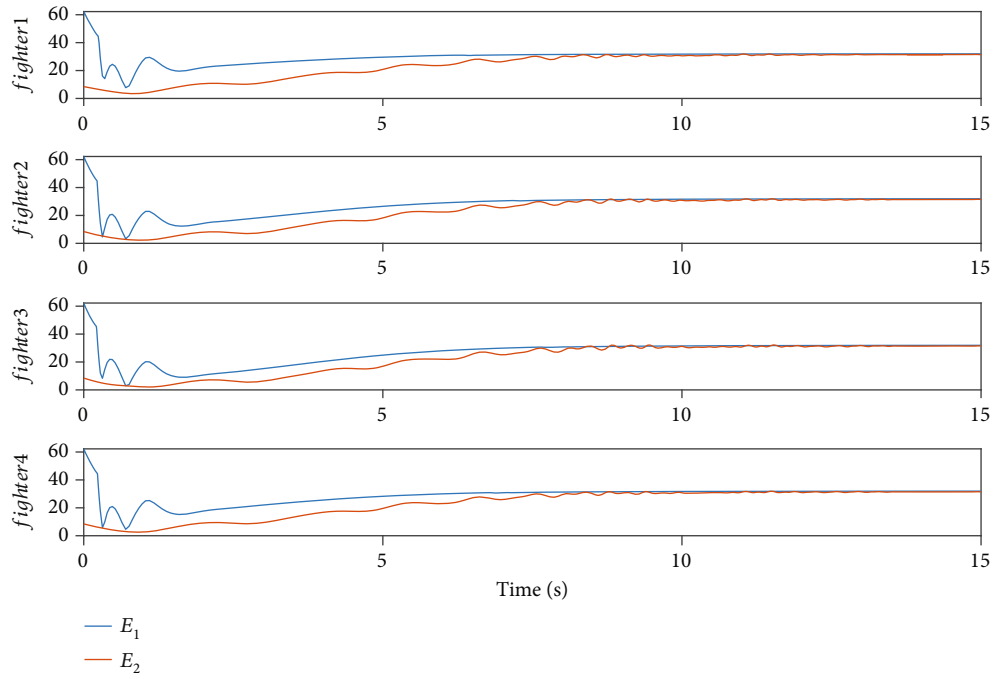

Figure 14: Actuator actions.

$$g_{k,1}(t, x_{k,1}) = -\begin{bmatrix} -1 & 0 & 0 \\ 0 & -1 & 0 \\ 0 & 0 & \cos\alpha_0 \end{bmatrix}, \tag{63}$$

$$f_{k,2}(t, \bar{x}_{k,2}) = q\cos\phi - r\sin\phi, \tag{64}$$

$$g_{k,2}(t, \bar{x}_{k,2}) = 0, \tag{65}$$

$$f_{k,3}(t, \bar{x}_{k,3}) = \begin{bmatrix} l_\beta\beta + l_p p + l_q q + l_r r + (l_{\beta\alpha}\beta + l_{r\alpha} r)\Delta\alpha - i_1 qr \\ m_\alpha\Delta\alpha + m_q q + i_2 pr - m_{\dot{\alpha}}\left(\frac{g_0}{V}\right)(\cos\theta\cos\phi - \cos\theta_0) \\ n_\beta\beta + n_r r + n_p p + n_{p\alpha} p\Delta\alpha - i_3 pq + n_q q \end{bmatrix}, \tag{66}$$

$$g_{k,3}(t, \bar{x}_{k,3}) = [L, M, N]^T, \tag{67}$$

$$L = \left[l_{\delta_{el}}, l_{\delta_{er}}, l_{\delta_{al}}, l_{\delta_{ar}}, 0, 0, l_{\delta_r}\right], \tag{68}$$

$$M = \left[m_{\delta_{el}}, m_{\delta_{er}}, m_{\delta_{al}}, m_{\delta_{ar}}, m_{\delta_{lef}}, m_{\delta_{tef}}, m_{\delta_r}\right], \tag{69}$$

$$N = \left[n_{\delta_{el}}, n_{\delta_{er}}, n_{\delta_{al}}, n_{\delta_{ar}}, 0, 0, n_{\delta_r}\right], \tag{70}$$

where $x_{k,1} = [\phi, \alpha, \beta]^{\mathrm{T}}$ is roll angle, attack angle, and sideslip angle, $x_{k,2} = \theta$ is pitch angle, $x_{k,3} = [p, q, \widehat{r}]^{\mathrm{T}}$ is roll angular velocity, pitching angular velocity, and yaw angular velocity, respectively. $u_k = [\delta_{el}, \delta_{er}, \delta_{al}, \delta_{ar}, \delta_{lef}, \delta_{tef}, \delta_r]^{\mathrm{T}}$ is left and right elevators, left and right ailerons, front and rear flaps, and rudder, respectively. The parameters and variables of this model are explained in detail in [34]. Assume that they are all flying at 40,000 feet, at 0.6 Mach. The expected roll angle, attack angle, and sideslip angle for the fighters are $y_d = [\phi_d, \alpha_d, \beta_d]^T$ with $\phi_d = 20°$, $\alpha_d = 30°$, $\beta_d = 0°$, respectively. The communication topology for the four fighters is shown in Figure 6.

The tracking errors are defined as $\phi_{k,e} = \phi_k - q_{d,1}$, $\alpha_{k,e} = \alpha_k - q_{d,2}$, and $\beta_{k,e} = \beta_k - q_{d,3}$, where $q_{d,1}$, $q_{d,2}$, and $q_{d,3}$ are the signals generated by (7), and $y_{d,i}$ is, respectively, the filter inputs. From $e_{k,1}(0) = [-16°, -25°, 0°]^T$, design $[\rho^0_{k,1}, \rho^0_{k,2}, \rho^0_{k,3}]^T = [20°, 33°, 3°]^T$ to satisfy $\rho^0_{k,i} > |e_{k,i}(0)|$. $[\rho^\infty_{k,1}, \rho^\infty_{k,2}, \rho^\infty_{k,3}]^T = [0.05°, 0.02°, 0.05°]^T$, and $[l_{k,1}, l_{k,2}, l_{k,3}]^T = [0.25, 0.25, 0.40]^T$.

Define $\xi_{k,1,1} = \phi_{k,e}/\rho_{1,1}$, $\xi_{k,1,2} = \alpha_{k,e}/\rho_{1,2}$, $\xi_{k,1,3} = \beta_{k,e}/\rho_{1,3}$, $\xi_{k,2,1} = (p_k - \nu_{k,2,1})/\rho_{2,1}$, $\xi_{k,2,2} = (q_k - \nu_{k,2,2})/\rho_{2,2}$, $\xi_{k,2,3} = (\widehat{r}_k - \nu_{k,2,3})/\rho_{2,3}$, $\bar{K}_{k,i} = \mathrm{diag}\{K_{k,i1}, K_{k,i2}, K_{k,i3}\}$, $r_{k,i,j} = \ln((1 + \xi_{i,j})/(1 - \xi_{i,j}))$, $k = 1, 2, 3, 4$, $i = 1, 2$, $j = 1, 2, 3$, and $\tilde{r}_{k,i} = [r_{k,i,1}, r_{k,i,2}, r_{k,i,3}]^T$, $i = 1, 2$. The proposed control scheme with prescribed performance is established as follows.

$$\begin{aligned} \nu_{k,2} &= -\bar{K}_{k,1}\tilde{r}_{k,1}, \\ u_k &= -\bar{K}_{k,2}\tilde{r}_{k,2}, \end{aligned} \tag{71}$$

where the control parameters are set as $K_{k,11} = 8$, $K_{k,12} = 5$, $K_{k,13} = 12$, $K_{k,21} = 4$, $K_{k,22} = 5$, $K_{k,23} = 1.8$, and $k = 1, 2, 3, 4$.

In addition, to emphasize the capacity of the proposed controller to deal with the deadzone with a $u - D(u)$ characteristic in the presence of nominal deviation from linear slopes, we consider the deadzone function (2) where $h_l = \mathrm{diag}\{0.80 + 0.2\sin(t), 0.70 + 0.2\cos(t), 0.75 + \sin(3t), 0.85 + \cos(0.5t), 0.90 + \sin(t), 0.70 + 0.2\cos(t), 0.80 + 0.4\sin(t)\}$ $h_r = \mathrm{diag}\{0.75 + 0.2\cos(t), 0.80 + 0.4\sin(t), 0.70 + 0.1\sin(2t), 0.85 + 0.2\cos(2t), 0.90 + 0.4\sin(t), 0.70 + 0.2\cos(2t)$

, $0.80 + 0.4 \sin(t)\}$, $b_l = -[0.7, 0.5, 0.3, 0.6, 0.8, 0.4, 0.5]^T$, and $b_r = [0.5, 0.5, 0.8, 0.6, 0.3, 0.4, 0.7]^T$.

In order to facilitate comparison, we exploit the method [6] under the same conditions. From [6], define $\tilde{e}_{k,i} = [e_{k,i,1}, e_{k,i,2}, e_{k,i,3}]^T$, $i = 1, 2$, and the control protocols are presented as follows

$$\begin{aligned} v_{k,2} &= -\bar{K}_{k,1}\tilde{e}_{k,1}, \\ u_k &= -\bar{K}_{k,2}\tilde{e}_{k,2}. \end{aligned} \tag{72}$$

To ensure the validity of the comparative practical example, $\bar{K}_{k,i}$ and $i = 1, 2$ are the same as our proposed methods.

The results are indicated in Figures 7–13. In Figures 7–9, the chain dotted curves represent the actuator responses under the method control of [6], and the solid curves represent the actuator responses under our proposed methods. It is observed from Figures 7–9 that control performance under our approach is fairly better than [6] since our roll angle, attack angle, and sideslip angle responses can be faster and more accurately trail the desired value. Figures 10–13 indicate the actions of actuators under the method of this paper. Figure 14 demonstrates the control performance of our approach and [6]. As shown in Figure 14, the blue curves represent the actuator efforts E_1 under our methodology, and the red curves represent the actuator efforts E_2 of [6], where E_1 and E_2 are defined as

$$E = \sqrt{\delta_{el}^2 + \delta_{er}^2 + \delta_{al}^2 + \delta_{ar}^2 + \delta_{lef}^2 + \delta_{tef}^2 + \delta_r^2}, \tag{73}$$

It is clear from the result presented in Figure 14 that at the beginning, the actuator actions of our approach are greater to that in [6], but eventually, the distinction of the efforts between our method and [6] is little. In other words, our method's control performance is better with the almost same control force.

The results that all the closed loop signals are bounded and the preset transient and steady state tracking performance are realized in the finite time can be concluded.

5. Conclusions

This paper investigates a distributed consensus control approach under a directed graph for a multiagent system with unknown input deadzone nonlinearities and time-varying control coefficients. To provide the required signals thus avoiding the estimation of the unknown matrix associated with the Laplace matrix, a two-order filter for each agent is established. Together with the two-order filter, a distributed prescribed performance control design was proposed for an uncertain heterogenous power-chained MAS with unknown input deadzone nonlinearities under a directed topology. This consensus control protocol is applied to two examples. Simulations results demonstrate the efficacy and advantage of the method.

Data Availability

The data used to support the findings of this study are available from the corresponding author upon request.

Conflicts of Interest

The authors declare that they have no conflicts of interest.

Acknowledgments

The work was supported by the National Natural Science Foundation of China (nos. 62176214, 61973253, and 62101590) and Natural Science Foundation of the Shaanxi Province, China (2021JQ-368).

References

[1] H. Su, G. Chen, X. Wang, and Z. Lin, "Adaptive second-order consensus of networked mobile agents with nonlinear dynamics," *Automatica*, vol. 47, no. 2, pp. 368–375, 2011.

[2] R. Cui, B. Ren, and S. Ge, "Synchronised tracking control of multi-agent system with high-order dynamics," *IET Control Theory & Applications*, vol. 6, no. 5, pp. 603–614, 2012.

[3] Z. Li, W. Ren, X. Liu, and M. Fu, "Consensus of multi-agent systems with general linear and Lipschitz nonlinear dynamics using distributed adaptive protocols," *IEEE Transactions on Automatic Control*, vol. 58, no. 7, pp. 1786–1791, 2013.

[4] M. Defoort, A. Polyakov, G. Demesure, M. Djemai, and K. Veluvolu, "Leader-follower fixed-time consensus for multi-agent systems with unknown non- linear inherent dynamics," *IET Control Theory & Applications*, vol. 9, no. 14, pp. 2165–2170, 2015.

[5] H. Zhang and F. L. Lewis, "Adaptive cooperative tracking control of higher-order nonlinear systems with unknown dynamics," *Automatica*, vol. 48, no. 7, pp. 1432–1439, 2012.

[6] J. Huang, W. Wang, C. Wen, J. Zhou, and G. Li, "Distributed adaptive leader-follower and leaderless consensus control of a class of strict-feedback nonlinear systems: a unified approach," *Automatica*, vol. 118, no. 5, article 109021, 2020.

[7] J. Zhou, Y. Wang, X. Zheng, Z. Wang, and H. Shen, "Weighted $${\mathcal {H}}_{\infty }$$ H ∞ consensus design for stochastic multi-agent systems subject to external disturbances and ADT switching topologies," *Nonlinear Dynamics*, vol. 96, no. 2, pp. 853–868, 2019.

[8] Y. Yang and D. Yue, "Distributed adaptive consensus tracking for a class of multi-agent systems via output feedback approach under switching topologies," *Neurocomputing*, vol. 174, pp. 1125–1132, 2016.

[9] Y. Wang and Y. Song, "Fraction dynamic-surface-based neuroadaptive finite-time containment control of multiagent systems in nonaffine pure-feedback form," *IEEE Transactions on Neural Networks and Learning Systems*, vol. 28, no. 3, pp. 678–689, 2017.

[10] C. L. P. Chen, G. X. Wen, Y. J. Liu, and Z. Liu, "Observer-Based adaptive backstepping consensus tracking control for high-order nonlinear semi-strict-feedback multiagent systems," *IEEE Transactions on Cybernetics*, vol. 46, no. 7, pp. 1591–1601, 2016.

[11] G. Wang, C. Wang, L. Li, and Z. Zhang, "Designing distributed consensus protocols for second-order nonlinear multi- agents

with unknown control directions under directed graphs," *Journal of the Franklin Institute*, vol. 354, no. 1, pp. 571–592, 2017.

[12] G. Wang, C. Wang, and Y. Shen, "Distributed adaptive leader-following tracking control of networked Lagrangian systems with unknown control directions under undirected/directed graphs," *International Journal of Control*, vol. 92, no. 12, pp. 2886–2898, 2019.

[13] C. P. Bechlioulis and G. A. Rovithakis, "Decentralized robust synchronization of unknown high order nonlinear multi-agent systems with prescribed transient and steady state performance," *IEEE Transactions on Automatic*, vol. 62, no. 1, pp. 123–134, 2017.

[14] H. J. Yang and D. Ye, "Adaptive fuzzy nonsingular fixed-time control for nonstrict-feedback constrained nonlinear multiagent systems with input saturation," *IEEE Transactions on Fuzzy Systems*, vol. 29, no. 10, pp. 3142–3153, 2021.

[15] C. Deng and G. Yang, "Distributed adaptive fuzzy control for nonlinear multiagent systems under directed graphs," *IEEE Transactions on Fuzzy Systems*, vol. 26, no. 99, pp. 1356–1366, 2018.

[16] G. Dong, H. Li, H. Ma, and R. Lu, "Finite-time consensus tracking neural network FTC of multi-agent systems," *IEEE Transactions on Neural Networks and Learning Systems*, vol. 32, no. 2, pp. 653–662, 2021.

[17] J. Huang, Y. Song, W. Wang, C. Wen, and G. Li, "Fully distributed adaptive consensus control of a class of high-order nonlinear systems with a directed topology and unknown control directions," *IEEE Transactions on Cybernetics*, vol. 48, no. 8, pp. 2349–2356, 2018.

[18] X. Yao and Y. Yang, "Adaptive fault compensation and disturbance suppression design for nonlinear systems with an aircraft control application," *International Journal of Aerospace Engineering*, vol. 2020, Article ID 4531302, 16 pages, 2020.

[19] C. Wang, C. Wen, and L. Guo, "Adaptive consensus control for nonlinear multiagent systems with unknown control directions and time-varying actuator faults," *IEEE Transactions on Automatic Control*, vol. 66, no. 9, pp. 4222–4229, 2021.

[20] W. Wang, C. Wen, J. Huang, and J. Zhou, "Adaptive consensus of uncertain nonlinear systems with event triggered communication and intermittent actuator faults," *Automatica*, vol. 111, article 108667, 2020.

[21] W. Wang and S. Tong, "Adaptive fuzzy bounded control for consensus of multiple strict-feedback nonlinear systems," *IEEE Transactions on Cybernetics*, vol. 48, no. 2, pp. 522–531, 2018.

[22] F. Liu, Y. Hua, X. Dong, Q. Li, and Z. Ren, "Adaptive fault-tolerant time-varying formation tracking for multi-agent systems under actuator failure and input saturation," *ISA Transactions*, vol. 104, pp. 145–153, 2020.

[23] Y. Hua, X. Dong, Q. Li, and Z. Ren, "Distributed fault-tolerant time-varying formation control for high-order linear multi-agent systems with actuator failures," *ISA Transactions*, vol. 71, pp. 40–50, 2017.

[24] G. Wang, C. Wang, and L. Li, "Fully distributed low-complexity control for nonlinear strict-feedback multiagent systems with unknown dead-zone inputs," *IEEE Transactions on Systems, Man, and Cybernetics: Systems*, vol. 50, no. 2, pp. 421–431, 2020.

[25] S. J. Yoo and T. H. Kim, "Decentralized low-complexity tracking of uncertain interconnected high-order nonlinear systems with unknown high powers," *Journal of the Franklin Institute*, vol. 355, no. 11, pp. 4515–4532, 2018.

[26] S. J. Yoo, "Approximation-free design for distributed consensus tracking of networked uncertain nonlinear multi-agent systems with heterogenous high powers," *IET Control Theory and Applications*, vol. 14, no. 14, pp. 1975–1988, 2020.

[27] J. M. Peng, J. N. Wang, and J. Y. Shan, "Robust cooperative output tracking of networked high-order power integrators systems," *International Journal of Control*, vol. 89, no. 2, pp. 270–280, 2016.

[28] H. Ma, D. Liu, D. Wang, and B. Luo, "Bipartite output consensus in networked multi-agent systems of high-order power integrators with signed digraph and input noises," *International Journal of Systems Science*, vol. 47, no. 13, pp. 3116–3131, 2016.

[29] W. Li, L. Liu, and G. Feng, "Cooperative control of multiple stochastic high-order nonlinear systems," *Automatica*, vol. 82, pp. 218–225, 2017.

[30] Y. Shang, B. Chen, and C. Lin, "Neural adaptive tracking control for a class of high-order non-strict feedback nonlinear multi-agent systems," *Neurocomputing*, vol. 316, pp. 59–67, 2018.

[31] S. J. Yoo, "A robust low-complexity tracker design with preassigned performance for uncertain high-order nonlinear systems with unknown time-varying delays and high powers," *Journal of the Franklin Institute*, vol. 355, no. 2, pp. 675–692, 2017.

[32] W. Wang, D. Wang, Z. Peng, and T. Li, "Prescribed performance consensus of uncertain nonlinear strict-feedback systems with unknown control directions," *IEEE Transactions on Systems, Man, and Cybernetics: Systems*, vol. 46, no. 9, pp. 1279–1286, 2016.

[33] E. D. Sontag, *Mathematical Control Theory: Deterministic Finite Dimensional Systems*, Springer Science & Business Media, Berlin, Germany, 2013.

[34] E. V. Oort, L. Sonneveldt, and Q. Chu, "Comparison of adaptive nonlinear control designs for an over-actuated fighter aircraft model," in *AIAA Guidance, Navigation and Control Conference and Exhibit*, pp. 18–21, Honolulu, USA, August 2008.